DEVELOPMENT OF A GAS DISTRIBUTION MEASURING SYSTEM FOR GAS SHEET BEAM PROFILE MONITOR

I. Yamada[1,†], Graduate School of Science and Engineering, Doshisha University, Kyoto, Japan
N. Ogiwara, Y. Hikichi, J. Kamiya, and M. Kinsho, [1]J-PARC center, Ibaraki, Japan

Abstract

The monitor system with sheet-shaped gas to non-destructively measure a two-dimensional transverse beam profile is under development. To obtain a correct beam profile, measurement of the gas density distribution is indispensable because the signal from the monitor is in proportional to both the beam intensity and the gas density distribution. A measurement system for three-dimensional gas distribution which detects ions produced by interaction between gas and electron beam has been developed. The system consists of an electron gun for producing ideal narrow beam, electrodes to form a parallel electric field toward a detector, a micro-channel plate and a phosphor screen. Measured ion distribution was well explained by considering the effects of the thermal velocity and the middle or viscos flow of the gas molecules.

INTRODUCTION

A non-destructive beam profile monitor is demanded in high intensity accelerator, like Japan Proton Accelerator Research Complex (J-PARC), because a solid-based beam profile monitor produces unallowable levels of the radiation. The beam profile monitors using residual gas in vacuum chamber have been developed [1]. However, the monitors still have some issues. One of the problems is that the signal is low due to ultra-low gas pressure in the accelerator chambers. Monitors with injected gas, like a gas jet monitor, are also being developed to solve the issue [2, 3].

We have been developing a gas sheet beam profile monitor to measure the transverse beam profile non-destructively in two dimensions [4, 5]. This monitor detects a beam profile using ions, electrons, or fluorescence produced by interaction between sheet-shaped gas and the beam. The gas sheet beam profile monitor gives the signal that is in proportion to the beam intensity distribution and the gas density distribution. One of the issues to utilize the monitor is inhomogeneous detection efficiency due to the non-uniformity of gas density distribution. To obtain the correct beam profile data, we have developed a gas distribution measuring system.

GAS DISTRIBUTION MEASURING SYSTEM

Concept of the gas distribution measuring system under development is shown in Fig. 1. This system measures the gas density distribution in three dimensions before installing the monitor in an accelerator. The system consists of a gas sheet that is a measuring object, an electron beam, and an electric field to transport ions produced by beam-

gas interaction to a detector. The electron beam produces ions when the beam passes through the gas sheet. One-dimensional gas distribution along the electron beam is obtained by transporting the ions to the detector. The gas distribution in three dimensions can be measured by scanning the gas sheet or the beam in x and y directions of Fig. 1.

In this system, if the ion trajectories overlap on the detector, the ionization position cannot be distinguished and the gas distribution cannot be measured. Therefore, electrodes to form a parallel electric field which transports the ions to the detector with keeping the relation of the ionization positions was designed. It is necessary to experimentally evaluate whether the ionization position can be distinguished. A proof-of-principle experiment was conducted with not a gas sheet but a narrow gas jet that plays a role as a part of the gas sheet (Fig. 2). The narrow gas plays a role of limiting ionization point. The relation between the ionization position and the detection position can be obtained by moving the gas nozzle position.
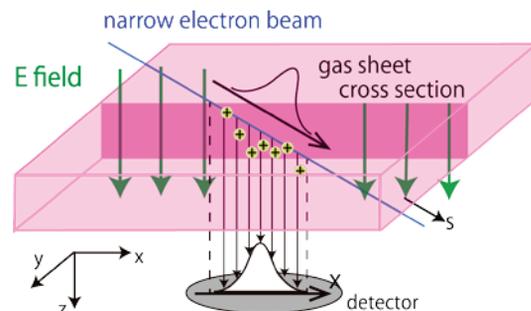

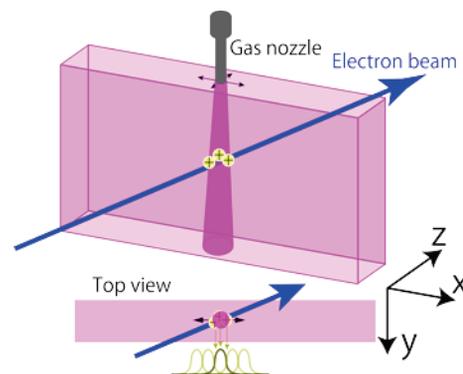Figure 1: Concept of the gas distribution measuring system.

Figure 2: Concept of the proof-of-principle experiment. Using a narrow gas jet instead of a gas sheet can limit the ionization position. The relation between the ionization position and the detection position can be obtained by moving the gas nozzle position.

† ip_yamada@icloud.com

MC6: Beam Instrumentation, Controls, Feedback and Operational Aspects

T03 Beam Diagnostics and Instrumentation

Before the measurement of the ionization and detection position relations, it is necessary to evaluate whether the detected signal itself which is affected by the size of the electron beam, distribution of the gas molecules, etc., is reliable. In this paper, first, we describe the experimental setup. Second, the detected image is shown. Finally, the validity of the detected signal is discussed.

THE EXPERIMENTAL SETUP

The setup of principle-proof experiment is shown in Fig. 3. The system consists of a narrow gas nozzle that is made of stainless steel tube with an inner diameter of 0.25 mm and a length of 65 mm, a 5 keV electron gun, electrodes that consists of copper meshes (wire diameter: 0.28 mm, pitch: 1.27 mm) and a cylinder electrode to form a parallel electric field, detectors that consists of a micro-channel plate (MCP) and a phosphor screen of 30 mm diameter, and a Faraday cup. Nitrogen gas is utilized because nitrogen is expected to have larger ionization cross section than Argon or Xenon [6]. The electric potential on each part is decided to form a parallel field only between the metal meshes and not to form fields between the lower mesh and the MCP. The ions produced by the beam-gas interaction are converted into electrons and amplified by the MCP. The produced ion signal is transported to the MCP and is amplified as a signal of electrons. The phosphor screen shows an image of the electrons. The image is taken photograph using Nikon D5500 (1300 px × 1300 px in 30 mm × 30 mm) in 14-bit dynamic range. The space resolution of detectors is 0.1 mm that is determined by the resolution of the MCP and the phosphor screen.

In this time, the gas nozzle position was fixed to inspect that the detected ion distribution is appropriate as a first step of the proof-of-principle experiment.
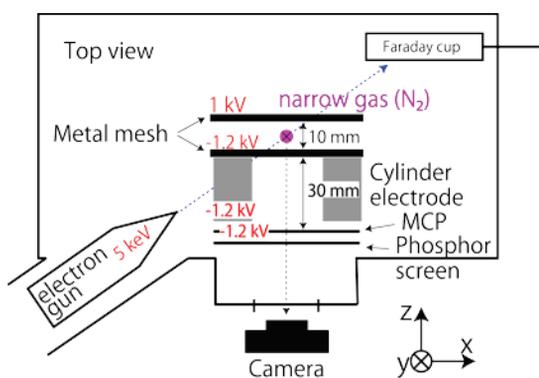

Figure 3: The setup of principle-proof experiment. The narrow gas flows from the front to the back.

DETECTED ION DISTRIBUTION AND EVALUATION

One of the images on the phosphor screen is shown in Fig. 4. This is the detected image when the pressure at the upsvtream of the gas nozzle (injection gas pressure) is 700 Pa. The background image without gas injection was already subtracted. The white line indicates the signal of the ions produced by the interaction between the electron beam

and the N_2 gas. This result means the electron beam can pass through the electrodes, but the electron beam is anticipated to distort. Although such distortion is not allowed in the three-dimensional measurement, it has no unwanted effect in the two-dimensional measurement with the narrow gas in the current case. The signal is analyzed along two kinds of axes to evaluate the effect of an electron beam profile and a gas distribution.
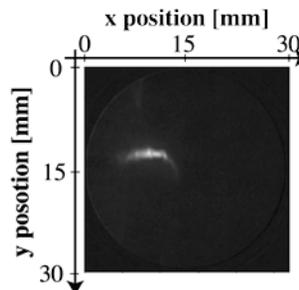

Figure 4: An image on the phosphor screen. The white line indicates the ion signal produced by interaction between the electron beam and the narrow gas.

The ion distribution of a cross section along the vertical (y) axis including the maximum intensity point in the phosphor screen is shown in Fig. 5. The intensity is in proportional to both the transverse profile of the electron beam and the narrow gas distribution along the nozzle axis. The beam profile was measured by a movable Faraday cup in advance using other setup, and the full width at half maximum (FWHM) was 0.27 mm. The gas distribution in the cross section area between the electron beam and the gas can be assumed to be uniform in such a small area. Therefore, the ion distribution in Fig. 5 should correspond to the electron beam distribution. However, the FWHM of the detected intensity distribution is 1.0 mm. Thermal velocity of the gas molecules may cause the difference in the FWHM. The ion distribution spreads by the thermal velocity worked as an initial velocity of the ions in the process of transport from the ionization point to the MCP. According to an ion trajectory simulation (CST studio [7]) included the thermal velocity effect, 0.27 mm in FWHM is detected as 1 mm of FWHM on the MCP (or the phosphor screen). This simulated result agrees with the experimental result.
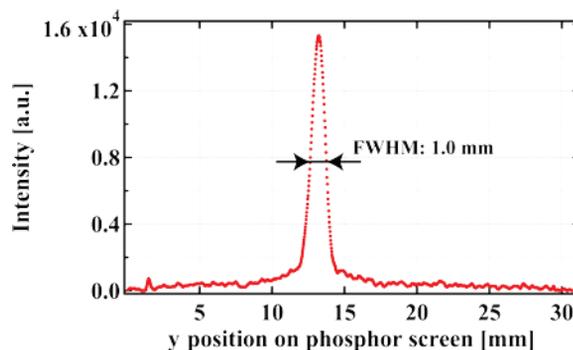

Figure 5: The ion distribution along the vertical axis, which includes the maximum intensity point in the phosphor screen.

Next, the validity of the detected signal is discussed from a viewpoint of the gas distribution. The ion distribution along the horizontal (x) axis in several injection gas pressure is shown in Fig. 6. The ion distribution along x axis should correspond to the gas distribution because the electron beam distribution is uniform along the x axis. To quantitatively discuss about the effect of the gas distribution based on the detected ion distribution, the peak intensity and the FWHM dependence on the injection gas pressure are shown in Fig. 7. The peak intensity is linear to the injection gas pressure. The FWHM in the region of the lower injection pressure is constant. Those mean that the intensity of the detected ion distribution is linear to the injection pressure at the lower pressure region. Those results also imply the shape of the ion distribution is independent on the injection pressure. On the other hand, the FWHM increases at the higher pressure region. This means the shape of the ion distribution changes to be wide with injection pressure. Thus, kinds of the gas flow changes with injection gas pressure. Here, to discuss the gas flow change, the gas flux of the nozzle dependence on the injection gas pressure is shown in Fig. 8. The gas flux can be divided into two regions, the linear and non-linear region. While the linear region of the gas flux is molecular flow region, the non-linear region is viscos or intermediate flow region. This result agrees with the results of Fig. 6 and Fig. 7.

The gas distribution in the molecular flow region was calculated with a Monte-Carlo simulation code, Molflow+ [8]. The ion distribution at 200 Pa injection is compared with a simulated gas distribution in Fig. 9. The simulated result is normalized at the peak of the experimental result. These distributions agree except the distribution tail. The causes of the difference in the distribution tail needs to be
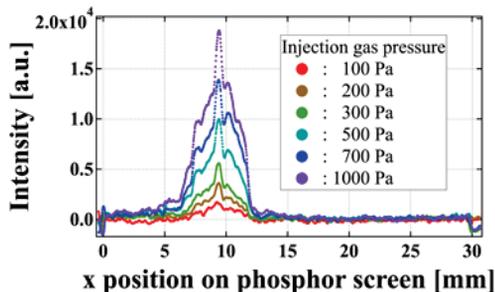
Figure 6: The ion distributions along the horizontal (x) axis at some conditions of the injection gas pressure.
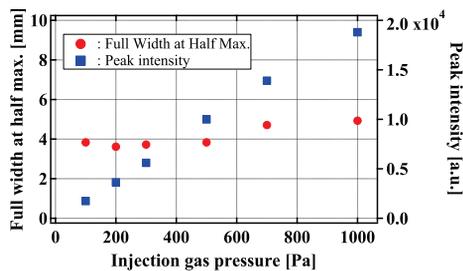
Figure 7: Variations of the FWHM and the peak intensity against the injection gas pressure.
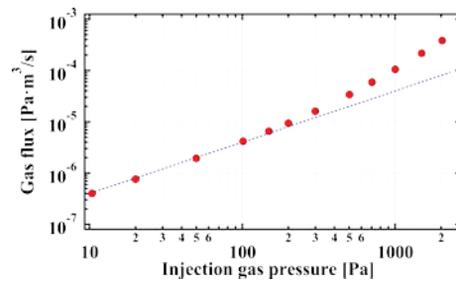
Figure 8: The characteristic of gas flux as a function of the injection gas pressure.

clarified because the tail is an important part to obtain the detection sensitivity of this system. One of the reasons is mismatch of the electron beam axis and the gas nozzle axis because the ionization area is the largest when these axes match. Hence, we can proceed the gas distribution measurement with the correct detection sensitivity including the tail of the signal by matching the gas jet and the electron beam axes.
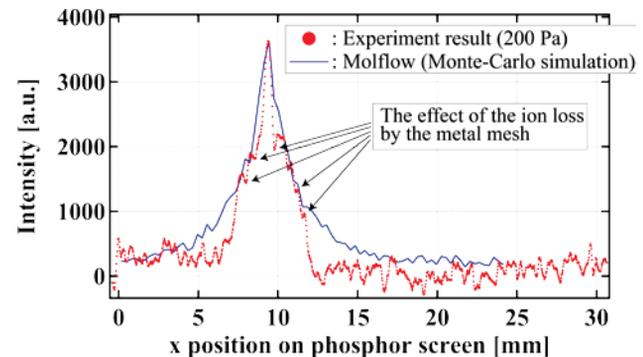
Figure 9: Comparing the experimental result with the Monte-Carlo simulation result (Molflow+).

CONCLUSION

The gas density distribution measuring system aimed at obtaining a sheet-shaped gas distribution of a new profile monitor has been developed. The results of the proof-of-principle experiment using the narrow gas instead of a gas sheet to confirm the ion trajectory agree with ion trajectory simulation and gas flow simulation. These results mean this system may be able to measure the gas distribution.

As the next step, the reaction of detection distribution peak position when the gas nozzle position changes will be inspected to obtain space resolution of this system. In addition, the 30 keV electron gun will be installed instead of the 5 keV gun to avoid distortion of the beam. Finally, a distribution of a sheet-shaped gas will be measured.

REFERENCES

[1] C. Andre, P. Forck, R. Haseitl, A. Reiter, R. Singh, and B. Walasek-Hoehne, "Optimization of Beam Induced Fluorescence Monitors for Profile Measurements of High Current Heavy Ion Beams at GSI", in *Proc. 3rd Int. Beam Instrumentation Conf. (IBIC'14)*, Monterey, CA, USA, Sep. 2014, paper TUPD05, pp. 412-416.

[2] V. Tzoganis, H. D. Zhang, A. Jeff, and C. P. Welsch, "Design and first operation of a supersonic gas jet based beam profile monitor", *Phys. Rev. Accel. Beams*, vol. 20, p. 062801, 2017. `doi:10.1103/PhysRevAcceBeams.20.062801`.

[3] Y. Hashimoto *et. al.*, "Oxygen gas-sheet beam profile monitor for the synchrotron and strage ring", *Nucl. Instrum. Method A*, vol. 527, p. 289, 2004.

`doi:10.1016/j.nima.2004.05.034`.

[4] N. Ogiwara, "Monte Carlo Simulation of Gas-sheet Targets Generated by Narrow Slits", *J. Vac. Soc. Jpn.,* vol. *56*, p.146, 2013.

[5] J. Kamiya, N. Ogiwara, A. Miura, M. Kinsho, and Y. Hikichi, "Non-destructive 2-D beam profile monitor using gas sheet in J-PARC LINAC", *J. Phys.: Conf. Ser.*, vol. 1067, p. 072006, 2018.

`doi:10.1088/1742-6596/1067/7/072006`.

[6] M. A. Plum, E. Bravin, J. Bosser, and R. Maccaferri, "N_2 and Xe gas scintillation cross-section, spectrum, and lifetime measurements from 50 MeV to 25 GeV at the CERN PS and Booster", *Nucl. Instrum. and Meth. A*, vol. 492, pp. 74-90, 2002.

`doi:10.1016/S0168-9002(02)01287-1`

[7] `https://www.aetjapan.com/software/CST_Overview.php`

[8] `https://molflow.web.cern.ch`